Hybrid Mesons, Multiquarks and Molecular States

Xiaoyan Shen, Ning Wu, Guofa Xu, Hu Qin, Shan Jin, Hong-Ying Jin, Shi-Lin Zhu
(Dated: November 3, 2006)

We give an overview of theoretical and experimental investigations of hybrid mesons, multiquarks and molecular states and discuss the search of them at BESIII.

PACS numbers:
Keywords: Hybrid Mesons, Multiquarks, Molecular States

I. INTRODUCTION

According to the constituent quark model (CQM), mesons and baryons are composed of $q\bar{q}$ and qqq respectively. CQM provides a convenient framework in the classification of hadrons. Most of experimentally observed hadron states fit into this scheme quite neatly. Any states beyond CQM are labelled as "non-conventional" hadrons.

However, CQM is only a phenomenological model. It's not derived from the underlying theory of the strong interaction—Quantum Chromodynamics (QCD). Hence the CQM spectrum is not necessarily the same as the physical spectrum in QCD, which remains ambiguous and elusive after decades of intensive theoretical and experimental exploration. No one is able to either prove or exclude the existence of these non-conventional states rigorously since nobody can solve the confinement issue in QCD now.

Hadron physicists generally take a modest and practical attitude. If one supposes these non-conventional states exist, then the important issues are: (1) How to determine their characteristic quantum numbers and estimate their masses, production cross-section and decay widths reliably? (2) How and in which channels to dig out the signal from backgrounds and identify them experimentally?

There are three classes of "non-conventional" hadrons. The first class are mesons with "exotic" J^{PC} quantum numbers. The possible angular momentum, parity and charge conjugation parity of a neutral $q\bar{q}$ meson are $J^{PC} = 0^{++}, 0^{-+}, 1^{++}, 1^{--}, 1^{+-}, \cdots$. In other words, a $q\bar{q}$ meson can never have $J^{PC} = 0^{--}, 0^{+-}, 1^{-+}, 2^{+-}, 3^{-+}, \cdots$. Any state with these "exotic" quantum numbers is clearly beyond CQM. We want to emphasize they are "exotic" only in the context of CQM. One can construct color-singlet local operators to verify that these quantum numbers are allowed in QCD. "Exotic" quantum numbers provide a powerful method for the experimental search of these "non-conventional" states. In contrast, a qqq baryon in CQM exhausts all possible J^P, i.e., $J^P = \frac{1}{2}^{\pm}, \frac{3}{2}^{\pm}, \frac{5}{2}^{\pm}, \cdots$.

The second class are hadrons with exotic flavor content. One typical example is the Θ^+ pentaquark. It was discovered in K^+n channel with the quark content $uudd\bar{s}$. Such a state is clearly beyond CQM. Exotic flavor content is also an asset in the experimental search of them.

The third class are hadrons which have ordinary quantum numbers but do not easily fit into CQM. Let's take the $J^{PC} = 0^{++}$ scalar mesons as an example. Below 2 GeV, we have $\sigma, f_0(980), f_0(1370), f_0(1500), f_0(1710), f_0(1790), f_0(1810)$. Within CQM there are only two scalars within this mass range if we ignore the radial excitations. With radial excitations, CQM could accommodate four scalars at most. Clearly there is serious overpopulation of the scalar spectrum. If all the above states are genuine, the quark content of some of them is not $q\bar{q}$. Overpopulation of the spectrum provides another useful window in the experimental search of non-conventional states.

Glueballs are hadrons composed of gluons. Quenched lattice QCD simulation suggests the scalar glueball is the lightest. Its mass is around $(1.5 \sim 1.7)$ GeV. Glueballs with the other quantum numbers are high-lying. In the large N_c limit, glueballs decouple from the conventional $q\bar{q}$ mesons [1]. Moreover, one gluon splits into two gluons freely in this limit. Hence the number of the gluon field inside glueballs is indefinite when $N_c \to \infty$. In the real world with $N_c = 3$, glueballs mix with nearby $q\bar{q}$ mesons with the same quantum numbers, which renders the experimental identification of scalar glueballs very difficult. Reviews of glueballs can be found in the previous chapters. In the following we discuss the other non-conventional hadrons according to their underlying quark gluon structure.

II. THEORETICAL MODELS FOR HYBRID MESONS

A. Large N_C expansion

Hybrid mesons are composed of a pair of $q\bar{q}$ and one explicit gluon field G. In the large N_c limit, the amplitude of creating a hybrid meson from the vacuum has the same N_c order as that of creating a $q\bar{q}$ meson [2]. If kinematics and other conservation laws allow, the production cross section of hybrid mesons is expected to be roughly the same as that of ordinary mesons. At least it's not suppressed in the large N_c limit. In the same limit, hybrid mesons and ordinary mesons mix freely if they carry the same quantum numbers. Hence, the identification of hybrid mesons is very difficult unless they have exotic quantum numbers. That's why so many efforts have been devoted to the search of the 1^{-+} hybrid

meson.

B. Flux tube model

The flux model is obtained intuitively in the strong coupling limit of lattice QCD [3, 4]. In this picture a meson is described as a pair of quark-antiquark linked by a color flux tube. The quarks move adiabatically in an effective potential generated by the flux tube dynamics. The orbital angular momentum along the flux tube is zero. The flux tube can also rotate along its axis. When the flux tube is in its ground state, the excitation of the quark-antiquark degree of freedom yields the conventional meson spectrum.

The hybrid mesons are defined as excitations of the color flux tube. The lowest-lying exotic hybrid meson is predicted to be with the quantum number $j^{PC} = 1^{-+}$ and a mass around 1.9 GeV [4], which is quite consistent with the prediction of the lattice QCD. The decay of a meson is triggered by breaking the flux tube in the flux tube model [3]. A quark-antiquark pair is assumed to be created with spin $S_{q\bar{q}} = 1$ and, orbital angular momentum $L_{q\bar{q}} = 1$ and total angular momentum $J_{q\bar{q}} = 0$. This process is called " $^3P_0$ pair creation". By the conservation of spin, a state with spin $S = 0$ can not decay into two $S = 0$ states [5]. The quark aniti-quark pair inside the lowest-lying 1^{-+} hybrid are the spin singlet in the flux tube model. Therefore it can not decay into a pair of spin zero mesons, such as $\pi\pi$,$\pi\eta$. Besides, when a flux tube is broken into two flux tubes (two mesons), since the relative coordinate of the two final flux tubes (the line connects the centers of the two flux tubes) is parallel to the original one (denoted as $\mathbf{r}$), the two final mesons cannot absorb the unit of string angular momentum about the $\mathbf{r}$ axis [3, 5] via their relative orbital angular momentum. Therefore the 1^{-+} hybrid (with one excited phonon polarized along the flux tube) cannot decay into two ground states, such as $\pi\pi$,$\pi\eta$ and $\pi\rho\cdots$. The preferential decay modes are those with one excited meson, such as $b_1\pi$, $f_1\pi\cdots$. This selection rule can be violated when the two final ground states have different spatial wave functions (i.e. they have different spatial size). One calculation shows that the partial width of $1^{-+} \to \rho\pi$ can be large and compatible with $\pi_1(1600)$ being a hybrid if the π shrinks to a point [6].

The original flux tube model (IKP model) was modified by introducing a new decay vertex. The vertex is constructed by using the heavy quark expansion of the Coulomb gauge QCD Hamiltonian to identify relevant operator [7, 8]. This new model (PSS model) extends the selection rule of IKP. PSS states that the decay amplitude of a hybrid meson vanishes when the daughter mesons are identical. This means that not only are the S+S-wave final states forbidden but also are the P+P-wave final states. The preferred channels are S+P-wave pairs. The prediction of the partial width of the 1^{-+} hybrid meson for each channel is also different as shown in Table I [8], where the mass of the 1^{-+} hybrid is set to be 1.6 GeV. It should be noticed that the width of $\rho\pi$ is bigger than that of $f_1\pi$ in PSS. An extensive study of the decay patterns of the hybrid mesons with other quantum numbers in the flux tube model are collected in the appendix, which was taken Ref. [8].

	$b_1\pi$	$\rho\pi$	$f_1\pi$	$\eta(1295)\pi$	K^*K
PSS(MeV)	24	9	5	2	0.8
IKP(MeV)	59	8	14	1	0.4

TABLE I: Decay widths of the 1^{-+} hybrid meson from the two flux tube model.

C. QCD sum rules

The mass and decay width of the 1^{-+} hybrid meson has been studied using QCD sum rules. Within this framework, one considers a two-point correlator

$$\Pi_{\mu\nu}(q^2) = i\int \mathrm{d}^4x\, \mathrm{e}^{iqx}\langle 0|T\{j_\mu(x), j_\nu^+(0)\}|0\rangle \quad (1)$$

where $j_\mu(x) = \bar{q}(x)T^a\gamma_\nu igG^a_{\mu\nu}q(x)$ is the interpolating current for the 1^{-+} isospin vector hybrid meson.

The spectral density $\rho_v(s) = \frac{1}{\pi}\mathbf{Im}\Pi_v(s)$ can be expressed in terms of the hybrid meson observables like its mass etc:

$$\frac{1}{\pi}\mathbf{Im}\Pi_v(s) = \sum_R M_R^6 f_R^2 \delta\left(s - M_R^2\right) + \text{QCD continuum}, \quad (2)$$

It can also be related to the correlator $\Pi_v(q^2)$ at the scale $-q^2$ via the dispersion relation

$$\Pi_{v,s}(q^2) = (q^2)^n \int_0^\infty ds \frac{\rho_v(s)}{s^n(s-q^2)} + \sum_{k=0}^{n-1} a_k (q^2)^k, \quad (3)$$

where the a_k are appropriate subtraction constants.

After invoking the Borel transformation to enhance the lowest-lying resonance in the spectral density, we have the QCD sum rules

$$R_k(\tau, s_0) = \int^{s_0} s^k \mathrm{e}^{-s\tau}\rho_v(s)\mathrm{d}s\ ;\ k = 0, 1, 2, \ldots \quad (4)$$

where the quantity R_k represents the QCD prediction, and s_0 is the threshold parameter.

The sum rules for 1^{-+} hybrid meson were obtained by various authors. The prediction for the hybrid mass is sensitive to the threshold s_0. The sum rule in the leading order of α_s expansion is unstable. When the next to leading order correction is included, the sum rule becomes more stable. It predicts the upper bound of 1^{-+} hybrid mass is 2.0 GeV [9].

	QCDSR	Flux Tube Model	PDG ($\pi_1(1600)$)
$b_1\pi$(MeV)	unstable	40 ± 20	seen
$f_1\pi$(MeV)	100	10 ± 5	seen
$\rho\pi$(MeV)	40 ± 20	9	seen
K^*K (MeV)	8	0.6	no
$\eta'\pi$ (MeV)	3	small	seen
$\eta\pi$ (MeV)	0.3	small	no

TABLE II: Comparison of the decay widths of the 1^{-+} hybrid meson from the flux tube model and QCD sum rule approach.

The decay widths of the 1^{-+} hybrid can be obtained by considering the three-point correlator

$$\Pi(p,q) = i \int \mathrm{d}^4x \mathrm{d}^4y \, \mathrm{e}^{ipx+iqy} \langle 0|T\{j_A(x) j_B(y) j_\mu(0)\}|0\rangle, \tag{5}$$

where $j_A(x)$ and $j_B(y)$ are operators which annihilate the final states A and B respectively.

When A and B are two pseudoscalars, $\Pi(p,q) = F_1(p+q)_\mu + F_2(p-q)_\mu$. Only F_2 is relevant to the process $1^{-+} \to AB$ and vanishes at the leading order [10]. At the next leading order, it was estimated [11]: $\Gamma(1^{-+} \to \pi\eta') \sim 3$MeV, $\Gamma(1^{-+} \to \pi\eta) \sim 0.3$MeV, which was quite consistent with the prediction from the flux tube model.

However, the channel $\pi\rho$ is not narrow from QCD sum rules approach. By using the three-point function at the symmetric point, the width of $1^{-+} \to \pi\rho$ was predicted in the region 250-600MeV [11, 12]. Later, it was pointed out that the calculation at the symmetric point receives large contamination from the high resonances and continnuum contribution [13]. By using the light-cone QCD sum rules and the double Borel transformation, the width is reduced to be 40 ± 20MeV [13]. The similar channel K^*K is suppressed by the kinematic space. The channel $f_1\pi$ is very broad (~ 100MeV) in QCD sum rules.

It is interesting to compare the prediction of the QCD sum rules with that of the flux tube model, although the bases of these two approaches are contradictory. The first one is based on the α_s expansion while the second one is based on the strong coupling expansion. From Table II , the decay patterns from these two approaches are very similar although the partial decay width for each channel is quite different:

$$\Gamma(f_1\pi) > \Gamma(\rho\pi) > \Gamma(K^*K) > \Gamma(\eta'\pi) > \Gamma(\eta\pi). \tag{6}$$

D. Comments

It's important to note that the gluon inside the hybrid meson can easily split into a pair of $q\bar{q}$. Therefore tetraquarks can always have the same quantum numbers as the hybrid mesons, including the exotic ones. Discovery of hadron candidates with $J^{PC} = 1^{-+}$ does not ensure it's an exotic hybrid meson. One has to exclude the tetraquark possibility based on its mass, decay width and decay pattern etc. This argument holds for $\pi_1(1400)$ and $\pi_1(1600)$.

The flux tube model predicts hybrid mesons prefer decaying into a pair of mesons with L=1 and L=0. Heavy hybrid mesons tend to decay into one P-wave heavy meson and one pseudoscalar meson according to a light-cone QCD sum rule calculation [14]. A lattice QCD simulation suggests the string breaking mechanism may play an important role for the decays of the hybrid heavy quarkonium [15]. When the string between the heavy quark and anti-quark breaks, new light mesons are created. In other words, the preferred final states are one heavy quarkonium plus light mesons. However, readers should be very cautious of these so-called "selection rules". None of them has been tested by experiments because none of the 1^{-+} hybrid candidates has been established unambiguously.

III. HUNTING FOR HYBRID MESONS AT BESIII/BEPCII

Hybrid mesons are color-singlet mixture of constituent quarks and gluons, such as $q\bar{q}g$ bound states. The evidence of the existence of the hybrid mesons is also a direct proof of the existence of the gluonic degree of freedom and the validity of QCD. The conventional wisdom is that it would be more fruitful to search for the low lying hybrid mesons with exotic quantum numbers than to search for glueballs. Hybrids have the additional attraction that, unlike glueballs, they span complete flavour nonets and hence provide many possibilities for experimental detection. In addition, the lightest hybrid multiplet includes at least one J^{PC} exotics.

In searching for hybrids, there are two ways to distinguish them from conventional states. One approach is to look for an access of observed states over the number predicted by the quark model. The drawback to this method is that it depends on a good understanding of hadron spectroscopy in a mass region that is still rather murky. At present, the phenomenological models have not been tested to the extent experimentally so that a given state can be reliably ruled out as a conventional meson. The situation is further muddied by expected mixing between conventional $q\bar{q}$ states and hybrids with the same J^{PC} quantum numbers. The other approach is to search for the states with quantum numbers that cannot be accommodated in the quark model. The discovery of exotic quantum numbers would be definite evidence of something new.

Who did the theoretical estimate? From the theoretical estimate, we know that $\Gamma(J/\psi \to MH) > \Gamma(J/\psi \to MM') > \Gamma(J/\psi \to MG)$, where M stands for ordinary a $q\bar{q}$ meson, G stands for a glueball and H stands for a hybrid. I.e., the J/ψ hadronic decay to hybrid states will have relatively large branching ratios and is an ideal place to study hybrid states and to search for exotic states.

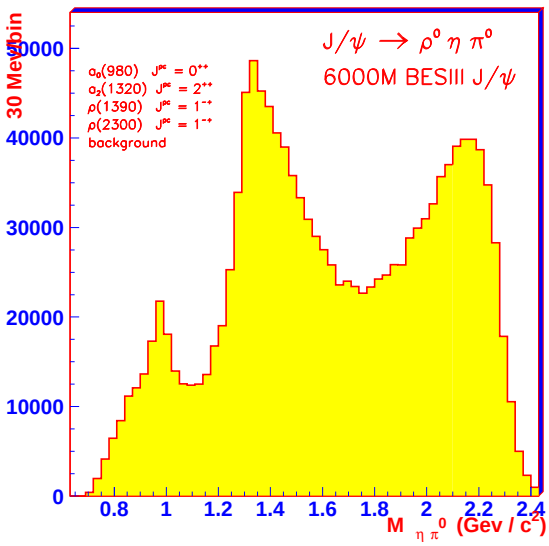

FIG. 1: The invariant mass spectrum of $\eta\pi^0$ in $J/\psi \to \rho\eta\pi^0$.

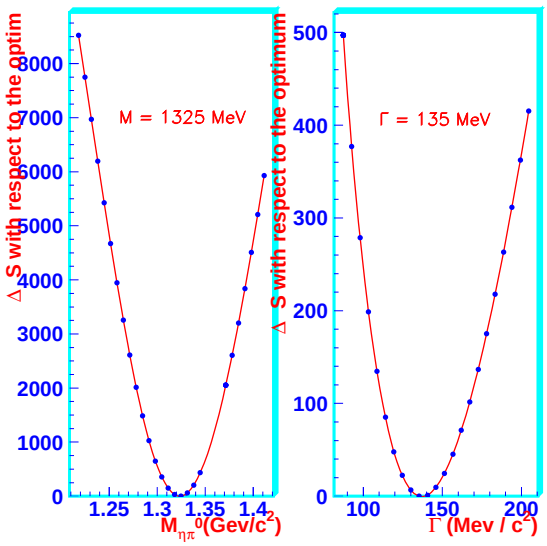

FIG. 2: The contribution of $a_2(1320)$ and the scan results of its mass and width.

Some previous experiments have searched for the 1^{-+} hybrid state $\pi_1(1400)$. Table III shows the list of the experiments searching for 1^{-+} resonances in $\eta\pi$ final states. All the experiments listed in Table III observed a clear forward-backward asymmetry and all of them except NICE suggested or claimed the evidence of an exotic $J^{PC} = 1^{-+}$ resonance. Of them, VES and E852 gave consistent results. From Crystal Barrels results on $\bar{p}d \to \eta\pi^-\pi^0 p$, the Dalitz plot is dominated by $\rho^- \to \pi^-\pi^0$ and there is a clear $\eta\pi$ P-wave which interferes with it. The fit to the Dalitz plot is improved when $\pi_1(1400)$ is included and the mass and width of $\pi_1(1400)$ are quite consistent with those from E852 experiment. E852 also found the evidence of another 1^{-+} exotic $\pi_1(1600)$, decaying to $\rho\pi$ in $\pi^- p \to \pi^-\pi^+\pi^- p$ reaction, with the mass and width being 1593 ± 8 MeV/c^2 and 168 ± 20 MeV/c^2. Tentative evidence was put forward by the VES collaboration in $\eta'\pi$ from $\pi^- N \to \pi^-\eta' N$ process. VES saw a broad but resonant P_+ wave near this mass. However the phase motion is not distinctive.

At BESIII/BEPCII, the decay of $J/\psi \to \rho\eta\pi$ can be studied to search for 1^{-+} exotic state. As an example, $6 \times 10^9 J/\psi \to \rho\eta\pi$ Monte Carlo events are generated to pass through BESIII detector. In the simulation, the possible $a_2(1320), 1^{-+}X(1390), a_0(980)$ and $1^{-+}X(2300)$, as well as background are considered. A partial wave analysis (PWA) is performed to analyze this channel. Fig. 1 shows the invariant mass spectrum of $\eta\pi$. In Fig. 2 , the contribution of $a_2(1320)$ and the scan results of its mass and width are plotted. The minimum of the scan curve gives the mass or width of this resonance. The $1^{-+}X(1390)$ component is shown in Fig. 3 . From this Monte Carlo study, we know that the angular distributions of $a_2(1320)$ and $1^{-+}X(1390)$ are very different due to their different spin-parities, even though the masses are in the same region. Partial wave analysis is able to separate components which have different spin-parities but at the same mass, when the statistics is enough and the resolution of the spectrum is good. With a large statistics, it is also possible to measure the phase motion of P-wave and so to give a more convincing evidence for the existence of a resonance.

Some phenomenological models predict that the dominant decay channels of exotic mesons are $\pi b_1(1235)$ and $\pi f_1(1285)$. The dominant decay channel of b_1 is $\omega\pi$ and the dominant decay channels of f_1 are $\eta\pi\pi$ and 4π. So, it seems that these exotic states should appear in the invariant mass spectrum of 5π or $\eta 3\pi$. If these exotic states are produced through $J/\psi \to \rho X$, then we had to study the following decay channels: $J/\psi \to \rho X, X \to \pi\omega\pi$, $J/\psi \to \rho X, X \to 5\pi$, $J/\psi \to \rho X, X \to \eta 3\pi$. In addition, we can study iso-scalar exotic mesons through the following channels: $J/\psi \to \omega X, X \to \pi\pi_1(1400), \pi_1(1400) \to \rho\pi$, ... Since there are lots of neutral and charged tracks in each channel, a large coverage of solid angle is necessary to preserve a high event selection efficiency. Good energy resolution for neutral and charged tracks is also required to accurately measure the mass and width of these exotic states.

IV. MULTIQUARKS

When N ($N \geq 4$) quarks/antiquarks are confined within a single MIT bag, a multiquark state is formed. The color structure within a multiquark state is complicated and not unique. It always has a component which

TABLE III: Previous experiments searching for the 1^{-+} hybrid meson.

Exps.	Lab.	Reaction	p_{beam} (GeV/c)	Year
NICE	IHEP	$\pi^- p \to \eta\pi^0 n$	40	1981
GAMS	CERN	$\pi^- p \to \eta\pi^0 n$	100	1988
BENKEI	KEK	$\pi^- p \to \eta\pi^- p$	6.3	1993
VES	IHEP	$\pi^- N \to \eta\pi^- X$	37	1993
E852	BNL	$\pi^- p \to \eta\pi^- p$	18	1997

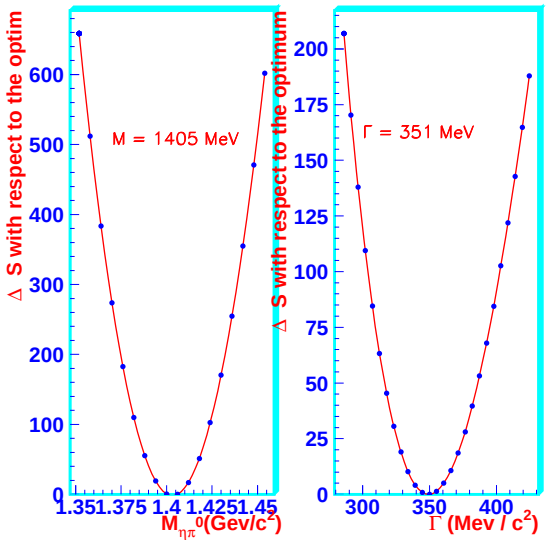

FIG. 3: The contribution of $\rho(1390)$ and the scan results of its mass and width.

is the product of two (or more) color-singlet hadrons. Special mechanism is needed to prevent the multiquark to fall apart easily and become extremely broad when it lies above threshold.

There are several well-known multiquark candidates. The first one is the H dibaryons suggested by Jaffe decades ago [16]. The on-going doubly-strange hypernuclei experiments have pushed its binding energy to be less than several MeV. Its existence is very dubious now. Jaffe also suggested that the low-lying scalar nonet are also tetraquarks because of their low mass and special mass pattern [17]. The third one is the fading Θ^+ pentaquark. Interested readers may consult the review [18]. **Dr S. Jin promised to finish the related BES part. Waiting.**

V. MOLECULAR STATES

Molecular states are bound states of two (or more) color-singlet hadrons. In other words, there are two (or more) MIT bags. Color-singlet hadrons are exchanged between these bags to produce the attractive force. Very often pions mediate the long-range interaction. There have been speculations of $f_0(980)$ being a $K\bar{K}$ molecule since it's only 10 MeV below $K\bar{K}$ threshold [19]. $\Lambda(1405)$ is sometimes postulated as a KN molecule.

[1] E. Witten, Nucl. Phys. B 169 (1979) 57.
[2] T. D. Cohen, Phys. Lett. B 427 (1998) 348.
[3] N. Isgur, R. Kokoski and J. Paton, Phys. Rev. Lett. 54 (1985) 869.
[4] N. Isgur and J. Paton, Phys. Rev. **D31** (1985) 2910.
[5] F. E. Close and P. R. Page, Nucl. Phys. **B443** (1995) 233.
[6] F. E. Close, J. J. Dudek, Phys. Rev. **D70** (2004) 094015.
[7] E. S. Swanson and A. P. Szczepaniak. Phys. Rev. **D56** (1997) 5692.
[8] P. R. Page, E. S. Swanson and A. P. Szczepaniak. Phys. Rev. **D59** (1999) 034016.
[9] H. Y. Jin, J. G. Korner and T. G. Steele, Phys. Rev. **D67** (2003) 014025.
[10] J. Govaerts *et al.*, Phys. Rev. Lett**53** (1984) 2207.
[11] J. I. Latorre, P. Pascual and S. Narison, Z. Phys. **C37**(1987) 347.
[12] S. Narison, QCD Spectral Sum Rules, Lecture Notes in Physics, Vol. 26, P368.
[13] S.-L. Zhu, Phys. Rev. **D60** (1999) 097502.
[14] S.-L. Zhu, Phys. Rev. D 60 (1999) 014008.
[15] G. S. Bali, Phys. Rev. D 71 (2005) 114513.
[16] R. L. Jaffe, Phys. Rev. Lett. 38 (1977) 195.
[17] R. L. Jaffe, Phys. Rev. D 15 (1977) 267.
[18] S.-L. Zhu, Int. J. Mod. Phys. A 19 (2004) 3439.
[19] J. Weinstein, N. Isgur, Phys. Rev. D 41 (1990) 2236.

TABLE IV: 2^{-+} Isovector Hybrid Decay Modes from Ref. [8].

			alt	high mass	standard	IKP	reduced
2^{-+}	$\rho\pi$	P	9	16	13	12	57
	K^*K	P	1	5	2	1	17
	$\rho\omega$	P	0	0	0	0	20
	$f_2(1270)\pi$	S	19	10	9	14	
		D	.1	.2	.05	11	
	$f_1(1285)\pi$	D	.1	.3	.06	Ø	
	$f_0(1370)\pi$	D	.02	.08	.01	.6	
	$b_1(1235)\pi$	D	Ø	Ø	Ø	20	
	$a_2(1320)\eta$	S	–	7	–	–	
		D	–	.01	–	–	
	$a_1(1260)\eta$	D	0	.05	0	0	
	$a_0(1450)\eta$	D	–	0	–	–	
	$K_2^*(1430)K$	S	–	11	–	–	
		D	–	0	–	–	
	$K_1(1270)K$	D	0	.01	0	.02	
	$K_0^*(1430)K$	D	–	0	–	–	
	$K_1(1400)K$	D	–	0	–	–	
	$\rho(1450)\pi$	P	.8	12	3	2	
	$K^*(1410)K$	P	–	1	–	–	
	Γ		30	63	27	59	

TABLE V: 1^{-+} Isovector Hybrid Decay Modes from Ref. [8].

			alt	high mass	standard	IKP	reduced
1^{-+}	$\eta\pi$	P	0	.02	.02	.02	99
	$\eta^{'}\pi$	P	0	.01	.01	0	30
	$\rho\pi$	P	9	16	13	12	57
	K^*K	P	1	5	2	1	17
	$\rho\omega$	P	0	0	0	0	13
	$f_2(1270)\pi$	D	.2	.5	.1	Ø	
	$f_1(1285)\pi$	S	18	10	9	14	
		D	.06	.2	.04	7	
	$b_1(1235)\pi$	S	78	40	37	51	
		D	2	3	1	11	
	$a_2(1320)\eta$	D	–	.02	–	–	
	$a_1(1260)\eta$	S	5	7	3	8	
		D	0	.01	0	.01	
	$K_2^*(1430)K$	D	–	0	–	–	
	$K_1(1270)K$	S	4	7	2	6	
		D	0	.2	0	.04	
	$K_1(1400)K$	S	–	33	–	–	
		D	–	0	–	–	
	$\pi(1300)\eta$	P	–	5	–	–	
	$\eta_u(1295)\pi$	P	3	27	11	8	
	$K(1460)K$	P	–	.8	–	–	
	$\rho(1450)\pi$	P	.8	12	3	2	
	$K^*(1410)K$	P	–	1	–	–	
	Γ		121	168	81	117	

TABLE VI: 1^{--} Isovector Hybrid Decay Modes from Ref. [8].

			alt	high mass	standard	IKP	reduced
1^{--}	$\omega\pi$	P	9	16	13	12	57
	$\rho\eta$	P	4	9	6	4	30
	$\rho\eta^{'}$	P	.1	1	.2	.1	1
	K^*K	P	3	9	5	3	34
	$a_2(1320)\pi$	D	.5	2	.3	16	
	$a_1(1260)\pi$	S	78	41	37	51	
		D	.4	.8	.2	11	
	$h_1(1170)\pi$	S			Ø		
		D			Ø		
	$b_1(1235)\eta$	S			Ø		
		D			Ø		
	$K_2^*(1430)K$	D	–	0	–	–	
	$K_1(1270)K$	S	6	12	4	11	
		D	0	.01	0	0	
	$K_1(1400)K$	S	–	17	–	–	
		D	–	0	–	–	
	$\omega(1420)\pi$	P	1	14	4	4	
	$K^*(1410)K$	P	–	3	–	–	
	Γ		103	121	70	112	

TABLE VII: 2^{+-} Isovector Hybrid Decay Modes from Ref. [8].

			alt	high mass	standard	IKP	reduced
2^{+-}	$\omega\pi$	D	.5	1	1	1	4
	$\rho\eta$	D	.1	.6	.2	.1	1
	$\rho\eta^{'}$	D	0	.02	0	0	0
	K^*K	D	.04	.2	.08	.04	.6
	$a_2(1320)\pi$	P	.7	.9	.4	130	
		F	0	.02	0	.2	
	$a_1(1260)\pi$	P	3	4	2	45	
		F	.01	.02	0	.3	
	$h_1(1170)\pi$	P	2	2	1	69	
		F	.01	.03	.01	.5	
	$b_1(1235)\eta$	P	.02	.5	.01	.8	
		F	0	0	0	0	
	$K_2^*(1430)K$	P	–	.04	–	–	
		F	–	0	–	–	
	$K_1(1270)K$	P	0	.03	0	.6	
		F	0	0	0	0	
	$K_1(1400)K$	P	–	.3	–	–	
		F	–	0	–	–	
	$\pi(1300)\pi$	D	.08	1	.2	.2	
	$\omega(1420)\pi$	D	.02	.4	.04	.04	
	$K^*(1410)K$	D	–	.01	–	–	
	Γ		7	11	5	248	

TABLE VIII: 0^{-+} Isovector Hybrid Decay Modes from Ref. [8].

			alt	high mass	standard	IKP	reduced
0^{-+}	$\rho\pi$	P	37	63	51	47	230
	K^*K	P	5	18	10	5	69
	$\rho\omega$	P			Ø		
	$f_2(1270)\pi$	D	1	3	.6	8	
	$f_0(1370)\pi$	S	62	40	30	62	
	$a_2(1320)\eta$	D	–	.1	–	–	
	$a_0(1450)\eta$	S	–	4	–	–	
	$K_2^*(1430)K$	D	–	.02	–	–	
	$K_0^*(1430)K$	S	–	44	–	–	
	$\rho(1450)\pi$	P	3	47	10	10	
	$K^*(1410)K$	P	–	5	–	–	
	Γ		108	224	102	132	

TABLE IX: 1^{+-} Isovector Hybrid Decay Modes from Ref. [8].

			alt	high mass	standard	IKP	reduced
1^{+-}	$\omega\pi$	S	23	19	26	38	118
		D	.3	.8	.4	.3	2
	$\rho\eta$	S	15	21	25	22	118
		D	.07	.3	.1	.06	.6
	$\rho\eta^{'}$	S	3	8	5	4	25
		D	0	.01	0	0	0
	K^*K	S	27	52	47	36	339
		D	.02	.1	.04	.02	.3
	$a_2(1320)\pi$	P	19	26	10	49	
		F	0	.02	0	.1	
	$a_1(1260)\pi$	P	9	10	5	29	
	$a_0(1450)\pi$	P	3	6	1	26	
	$h_1(1170)\pi$	P	Ø	Ø	Ø	95	
	$b_1(1235)\eta$	P	Ø	Ø	Ø	1	
	$K_2^*(1430)K$	P	–	1	–	–	
		F	–	0	–	–	
	$K_1(1270)K$	P	.04	.6	.02	5	
	$K_0^*(1430)K$	P	–	.4	–	–	
	$K_1(1400)K$	P	–	.4	–	–	
	$\omega(1420)\pi$	S	16	82	58	79	
		D	.01	.2	.02	.02	
	$K^*(1410)K$	S	–	110	–	–	
		D	–	.01	–	–	
	Γ		115	338	177	384	

TABLE X: 0^{+-} Isovector Hybrid Decay Modes from Ref. [8].

			alt	high mass	standard	IKP	reduced
0^{+-}	$a_1(1260)\pi$	P	Ø	Ø	Ø	309	
	$h_1(1170)\pi$	P	47	45	24	37	
	$b_1(1235)\eta$	P	.6	12	.4	.3	
	$K_1(1270)K$	P	.7	10	.4	7	
	$K_1(1400)K$	P	–	1	–	–	
	$\pi(1300)\pi$	S	60	246	222	312	
	$K(1460)K$	S	–	115	–	–	
	Γ		108	429	247	665	

TABLE XI: 1^{++} Isovector Hybrid Decay Modes from Ref. [8].

			alt	high mass	standard	IKP	reduced
1^{++}	$\rho\pi$	S	23	19	26	38	116
		D	1	3	2	1	8
	K^*K	S	14	26	24	18	170
		D	.04	.3	.09	.04	.6
	$\rho\omega$	S	0	0	0	0	47
		D	0	0	0	0	.03
	$f_2(1270)\pi$	P	4	5	2	75	
		F	.01	.03	0	.3	
	$f_1(1285)\pi$	P	7	9	4	62	
	$f_0(1370)\pi$	P	Ø	Ø	Ø	4	
	$b_1(1235)\pi$	P	Ø	Ø	Ø		
	$a_2(1320)\eta$	P	–	.9	–	–	
		F	–	0	–	–	
	$a_1(1260)\eta$	P	.2	3	.09	1	
	$a_0(1450)\eta$	P	–	Ø	–	–	
	$K_2^*(1430)K$	P	–	.4	–	–	
		F	–	0	–	–	
	$K_1(1270)K$	P	.07	1	.05	1	
	$K_0^*(1430)K$	P	–	0	–	–	
	$K_1(1400)K$	P	–	.7	–	–	
	$\rho(1450)\pi$	S	14	80	50	66	
		D	.02	.6	.05	.04	
	$K^*(1410)K$	S	–	55	–	–	
		D	–	.01	–	–	
	Γ		63	204	108	269	

TABLE XII: Isoscalar Hybrid Decay Modes from Ref. [8].

			alt	high mass	standard	IKP	reduced
2^{-+}	K^*K	P	1	5	2	1	17
	$a_2(1320)\pi$	S	52	31	25	45	
		D	.2	.6	.1	22	
	$a_1(1260)\pi$	D	.5	1	.3	Ø	
	$a_0(1450)\pi$	D	.02	.1	.01	.6	
	$f_2(1270)\eta$	S	–	8	–	–	
		D	–	.02	–	–	
	$f_1(1285)\eta$	D	–	.02	–	–	
	$f_0(1370)\eta$	D	–	0	–	–	
	$K_2^*(1430)K$	S	–	11	–	–	
		D	–	0	–	–	
		G	–	0	–	–	
	$K_1(1270)K$	D	0	.01	0	0	
	$K_0^*(1430)K$	D	–	0	–	–	
	$K_1(1400)K$	D	–	0	–	–	
	$K^*(1410)K$	P	–	1	–	–	
	Γ		54	58	27	69	
1^{-+}	$\eta^{'}\eta$	P	0	0	0	0	10
	K^*K	P	1	5	2	1	17
	$a_2(1320)\pi$	D	.4	1	.2	Ø	
	$a_1(1260)\pi$	S	59	30	28	38	
		D	.3	.6	.2	34	
	$f_2(1270)\eta$	D	–	.05	–	–	
	$f_1(1285)\eta$	S	–	8	–	–	
		D	–	.01	–	–	
	$K_2^*(1430)K$	D	–	0	–	–	
	$K_1(1270)K$	S	4	7	2	7	
		D	0	.2	0	0	
	$K_1(1400)K$	S	–	33	–	–	
		D	–	0	–	–	
	$\pi(1300)\pi$	P	8	65	27	27	
	$\eta_u(1295)\eta$	P	–	6	–	–	
	$K(1460)K$	P	–	.8	–	–	
	$K^*(1410)K$	P	–	1	–	–	
	Γ		73	158	59	107	
0^{-+}	K^*K	P	5	18	10	5	69
	$a_2(1320)\pi$	D	2	6	1	16	
	$a_0(1450)\pi$	S	145	114	70	175	
	$f_2(1270)\eta$	D	–	.2	–	–	
	$f_0(1370)\eta$	S	–	23	–	–	
	$K_2^*(1430)K$	D	–	.02	–	–	
	$K_0^*(1430)K$	S	–	44	–	–	
	$K^*(1410)K$	P		5			
	Γ		152	210	81	196	
1^{--}	$\rho\pi$	P	28	47	38	35	172
	$\omega\eta$	P	3	9	6	4	29
	$\omega\eta^{'}$	P	.1	1	.2	.3	.8
	K^*K	P	3	9	5	3	35
	$b_1(1235)\pi$	S	Ø	Ø	Ø		
		D			Ø		
	$h_1(1170)\eta$	S				Ø	
	$K_2^*(1430)K$	D	–	0	–	–	
	$K_1(1270)K$	S	6	12	4	11	
		D	0	.01	0	0	
	$K_1(1400)K$	S	–	17	–	–	

TABLE XIII: $s\bar{s}$ Hybrid Decay Modes from Ref. [8].

			alt	high mass	standard	IKP	reduced
2^{-+}	K^*K	P	6	13	11	8	82
	$K_2^*(1430)K$	S	28	29	21	44	
		D	.03	.5	.02	1	
	$K_1(1270)K$	D	.2	.5	.1	10	
	$K_0^*(1430)K$	D	.02	.3	.01	.2	
	$K_1(1400)K$	D	.06	.5	.03	.6	
	$f_2^{'}(1525)\eta$	S	–	20	–	–	
		D	–	.2	–	–	
	$f_1(1510)\eta$	D	–	.03	–	–	
	$f_0(1370)\eta$	D	.01	.08	0	.1	
	$K^*(1410)K$	P	2	27	6	5	
	Γ		36	91	38	69	
1^{-+}	$\eta^{'}\eta$	P	0	0	0	0	44
	K^*K	P	6	13	11	8	82
	$K_2^*(1430)K$	D	.07	1	.04	Ø	
	$K_1(1270)K$	S	14	10	11	14	
		D	3	8	2	21	
	$K_1(1400)K$	D	83	76	61	121	
		D	.03	.2	.02	.4	
	$f_2^{'}(1525)\eta$	D	–	.04	–	–	
	$f_1(1510)\eta$	S	–	21	–	–	
		D	–	.02	–	–	
	$K(1460)K$	P	1	45	4	3	
	$\eta_s(1490)\eta$	P	–	15	–	–	
	$K^*(1410)K$	P	2	27	6	5	
	Γ		109	216	95	172	
0^{-+}	K^*K	P	26	52	46	33	330
	$K_2^*(1430)K$	D	.4	6	.2	1	
	$K_0^*(1430)K$	S	113	117	83	174	
	$f_2^{'}(1525)\eta$	D	–	.2	–	–	
	$f_0(1370)\eta$	S	72	105	64	109	
	$K^*(1410)K$	P	7	110	22	18	
	Γ		218	390	215	335	
1^{--}	K^*K	P	13	26	23	16	165
	$\phi\eta$	P	2	19	11	3	89
	$\phi\eta^{'}$	P	.01	2	.1	.02	.5
	$K_2^*(1430)K$	D	.1	2	.07	2	
	$K_1(1270)K$	S	23	16	18	24	
		D	.2	.6	.1	2	
	$K_1(1400)K$	S	43	40	32	63	
		D	.1	.6	.04	.7	
	$h_1(1380)\eta$	S			Ø		
		D			Ø		
		D	.07	.6	.04	.3	
	$K^*(1410)K$	P	3	55	11	9	
	Γ		84	155	95	120	
2^{+-}	K^*K	D	1	3	2	1	13
	$\phi\eta$	D	.06	.8	.3	.08	2
	$\phi\eta^{'}$	D	0	0	0	0	0
	$K_2^*(1430)K$	P	.3	1	.2	32	
		F	0	.03	0	.01	
	$K_1(1270)K$	P	.2	.3	.1	17	
		F	.04	.2	.02	.6	
	$K_1(1400)K$	P	3	8	2	28	
		F	0	0	0	0	

TABLE XIV: $c\bar{c}$ Hybrid Decay Modes from Ref. [8].

			alt	high mass	standard	IKP	reduced
2^{-+}	D^*D	P	.5	.1	.8	4	19
	$D^{**}(2^+)D$	S	–	9	–	–	
		D	–	.2	–	–	
	$D^{**}(1^+_L)D$	D	–	.2	–	–	
	$D^{**}(0^+)D$	D	–	.2	–	–	
	$D^{**}(1^+_H)D$	D	–	.2	–	–	
	Γ		.5	10	.8	4	
1^{-+}	D^*D	P	.5	.1	.8	4	19
	$D^{**}(2^+)D$	D	–	.5	–	–	
	$D^{**}(1^+_L)D$	S	–	1.2	–	–	
		D	–	2.5	–	–	
	$D^{**}(1^+_H)D$	S	–	25	–	–	
		D	–	0	–	–	
	Γ		.5	29	.8	4	
0^{-+}	D^*D	P	2	.3	3	16	76
	$D^{**}(2^+)D$	D	–	2.5	–	–	
	$D^{**}(0^+)D$	S	–	25	–	–	
	Γ		2	28	3	16	
1^{--}	D^*D	P	1	.2	1.5	8	38
	$D^{**}(2^+)D$	D	–	1	–	–	
	$D^{**}(1^+_L)D$	S	–	7	–	–	
		D	–	.3	–	–	
	$D^{**}(1^+_H)D$	S	–	10	–	–	
		D	–	.2	–	–	
	Γ		1	19	1.5	8	
2^{+-}	D^*D	D	.2	.2	.3	1	7
	$D^{**}(2^+)D$	P	–	.5	–	–	
		F	–	.02	–	–	
	$D^{**}(1^+_L)D$	P	–	0	–	–	
		F	–	0	–	–	
	$D^{**}(1^+_H)$D	P	–	3	–	–	
		F	–	0	–	–	
	Γ		.2	4	.3	1	
1^{+-}	D^*D	S	.3	.1	.5	8	12
		D	.1	.1	.1	.5	4
	$D^{**}(2^+)D$	P	–	13	–	–	
		F	–	.01	–	–	
	$D^{**}(1^+_L)D$	P	–	2	–	–	
	$D^{**}(0^+)D$	P	–	8	–	–	
	$D^{**}(1^+_H)D$	P	–	2.5	–	–	
	Γ		.4	26	.6	8.5	
0^{+-}	$D^{**}(1^+_L)D$	P	–	25	–	–	
	$D^{**}(1^+_H)D$	P	–	15	–	–	
	Γ		–	40	–	–	
1^{++}	D^*D	S	.2	.1	.3	1	6
		D	.2	.2	.3	.3	8
	$D^{**}(2^+)D$	P	–	5	–	–	
		F	–	.03	–	–	
	$D^{**}(1^+_L)D$	P	–	5	–	–	
	$D^{**}(0^+)D$	P	–	Ø	–	–	
	$D^{**}(1^+_H)D$	P	–	5	–	–	
	Γ		.4	15	.6	1.3	